

Light scattering studies of the gelation process in an aqueous system of a non-ionic polymer and a cationic surfactant

Bo Nyström* and Jaan Roots

Department of Chemistry, The University of Oslo, PO Box 1033, Blindern, N-0315 Oslo 3, Norway

and Anders Carlsson† and Björn Lindman

Physical Chemistry 1, Chemical Center, Lund University, PO Box 124, S-221 00 Lund, Sweden

(Received 5 June 1991; revised 21 August 1991; accepted 2 October 1991)

Static and dynamic light scattering studies are presented on the temperature induced sol-gel transition of an aqueous system of the non-ionic cellulose derivative ethyl hydroxyethyl cellulose in the presence of a cationic surfactant. In dilute solution coil expansion is observed with increasing temperature. In the semidilute range structural changes of the network are found when approaching the sol-gel transition. These effects are explained by an enhanced binding of surfactant to the polymer. The relaxation of the correlation function, in the semidilute regime, is shifted towards longer times as the gelation threshold is approached. These results are interpreted in the framework of a model that has been constructed with the aid of the theoretical approach of Semenov. In this model the correlation function initially decays by a fast cooperative mode (single exponential), followed by a non-exponential decay (reptation-like mode) at longer times. The cooperative relaxation time is only slightly influenced by temperature, whereas the reptation-like relaxation time exhibits a drastic increase during the gelation process. This effect is attributed to a slowing down of the motion of the individual chains in the gelation zone. Within the framework of the model the determination of the gel point seems possible.

(Keywords: static light scattering; dynamic light scattering; ethyl hydroxyethyl cellulose; surfactant; aqueous solution; gel; sol-gel transition)

INTRODUCTION

It is well established¹⁻⁴ that the interaction between certain non-ionic polymers and ionic surfactants may give rise to a substantial increase in the viscosity of solutions, even at fairly low polymer concentration. Aqueous solutions of ethyl hydroxyethyl cellulose (EHEC) in the presence of the cationic surfactant cetyltrimethylammonium bromide (CTAB) constitute such a system⁵⁻⁸. In the semidilute regime, where the polymer molecules overlap each other and form a transient network, this system exhibits a temperature induced sol-gel transition. Upon heating, this system undergoes a transformation, at around 40–50°C depending on the degree of substitution of the polymer, from a solution to a clear physically cross-linked thermoreversible gel^{7,8}. The position and width of the gel transition zone is a function of, for example, the molecular weight of the polymer, surfactant concentration, type of surfactant and degree and heterogeneity of substitution. The mechanism of gelation is believed^{7,8} to be governed by an enhanced cooperative binding of ionic surfactant to the EHEC polymer with increasing temperature. The surmise is that during the process small micelle-like aggregates are

produced, which act as junction zones between hydrophobic segments of different polymer chains, giving rise to a physically cross-linked polymer network. Since these gels are completely transparent, light scattering constitutes a powerful tool to survey static and dynamic properties of this system.

Although, there is a vast amount of literature dealing with structural, dynamic and rheological features of polymeric gels, the number of studies concerning static and dynamic behaviour of polymer systems in the transition zone is rather limited. In order to gain a deeper understanding of this type of phenomenon we have carried out intensity and dynamic light scattering (d.l.s.) measurements on the system EHEC/CTAB/water, over an extended temperature range (25–51°C).

The intensity light scattering results reveal significant structural changes of the polymer network during the gelation process. When it comes to the results of the d.l.s. measurements, the relaxation of the monitored correlation function is found to be shifted towards longer times when the gel transition regime is approached. A tentative model, inspired by the theoretical approach of Semenov⁹, is advanced for the interpretation of the correlation function data. The picture that emerges is that the correlation function may be described by two different relaxation stages: a cooperative mode (short times) and a long-lived relaxation mode associated with reptation-like motions.

* To whom correspondence should be addressed

† Present address: Karlshamns LipidTeknik AB, PO Box 15200, S-104 65 Stockholm, Sweden

THEORETICAL BACKGROUND

We will briefly outline some theoretical aspects which will guide us in the interpretation of the intensity and d.l.s. results. In analysing data it is important to distinguish between the dilute and the semidilute regimes. In dilute solution the polymer molecules act as individual entities. As the concentration increases the overlap threshold concentration c^* is attained, which separates the dilute from the semidilute region^{10,11}. The transition concentration may be estimated from $c^* = 1/[\eta]$, where $[\eta]$ is the intrinsic viscosity. A semidilute solution may be pictured as a three-dimensional transient network with a characteristic length ξ (the screening length) which is related to the average distance between contact points (mesh size of the network)¹⁰.

Static light scattering

Intensity light scattering measurements may provide information about structural and thermodynamic properties of polymer systems. In a static light scattering experiment, the incident beam at wavelength λ impinges on a sample and is scattered into a detector placed at an angle θ with respect to the transmitted beam, and the intensity of the scattered light is measured. The magnitude of the scattering vector q is:

$$q = (4\pi n/\lambda) \sin(\theta/2) \quad (1)$$

where n is the refractive index of the medium. At low q in the dilute region the reduced inverse light scattering function may be written as:

$$\frac{Hc}{R_{VV}(c, q)} = \frac{1}{M} \left(1 + \frac{q^2 R_G^2}{3} \right) + 2A_2c + \dots \quad (2)$$

where H is an optical constant defined by:

$$H = (4\pi^2 n^2 / N_A \lambda^4) (\partial n / \partial c)^2 \quad (3)$$

with c , $R_{VV}(c, q)$, M , R_G , A_2 , N_A , and $\partial n / \partial c$ being, respectively, the mass concentration (mass/volume), the Rayleigh ratio for vertically polarized incident and vertically polarized scattered light, molecular weight of the solute, the root mean square radius of gyration, the second virial coefficient, Avogadro's number, and the refractive index increment. In terms of the normalized scattered intensity function we arrive at¹¹:

$$\frac{S(c, 0)}{S(c, q)} \approx 1 + \frac{q^2 R_G^2}{3} \quad (4)$$

where $S(c, q) \equiv R_{VV}(c, q)/(HcM)$ and

$$S(c, 0) = \frac{RT}{M(\partial\pi/\partial c)} = \frac{1}{1 + 2A_2Mc + \dots} \quad (5)$$

with R the gas constant and $(\partial\pi/\partial c)$ the inverse osmotic compressibility. Relation (4) is based on the Debye function which generally works well¹² for coil polymers at $q^2 R_G^2 < 10$.

In the semidilute regime the pair correlation function $g(r)$ of polymer segments is expected to follow an Ornstein-Zernike form in the intermediate range of r as¹⁰:

$$g(r) \approx (1/r) \exp(-r/\xi) \quad (l < r < R_G) \quad (6)$$

where l is the persistence length. The scattered intensity function (which is the Fourier transform of $g(r)$) has a Lorentzian form and the normalized inverse scattering

intensity function may be expressed as¹¹:

$$\frac{S(c, 0)}{S(c, q)} = 1 + \xi^2 q^2 \quad (7)$$

The intensity scattering function applies for the range of scattering vectors $R_G^{-1} < q < l^{-1}$. The form of equation (7) has been verified by small angle neutron scattering¹³, light scattering¹⁴ and X-ray scattering¹⁵ experiments.

Dynamic light scattering

Dynamic light scattering probes the dynamics of concentration and density fluctuations in polymer systems. The intensity of scattered light is measured as a function of time at a particular scattering angle and the normalized intensity autocorrelation function $g^{(2)}(t)$ is determined. This parameter is related to the first-order electric field correlation function $g^{(1)}(t)$, which is the theoretically tractable function, by the Siegert¹⁶ expression:

$$g^{(2)}(t) = 1 + B|g^{(1)}(t)|^2 \quad (8)$$

where B is usually treated as an empirical factor. For a polydisperse system, or if the correlation function representing a semidilute solution and/or gel is characterized by a distribution of relaxation times due to competing relaxation processes, the quantity $g^{(1)}(t)$ may be described by a Fredholm¹⁷ integral equation (of the first kind):

$$g^{(1)}(t) = \int_0^\infty \kappa(\tau) \exp(-t/\tau) d\tau \quad (9)$$

with

$$\int_0^\infty \kappa(\tau) d\tau = 1 \quad (10)$$

where $\kappa(\tau)$ is the distribution of relaxation times τ . In principle the data analysis consists of inverting the Laplace transformation (equation (9)). However, $g^{(1)}(t)$, evaluated from experimental data, is marred by noise and is usually bandwidth limited. Thus, the Laplace inversion of equation (9) is an ill-conditioned problem. These factors restrict the amount of information of $\kappa(\tau)$ that can be retrieved from $g^{(1)}(t)$. Several approximate procedures for treating equation (9) have been devised, e.g. the method of cumulants¹⁸, the histogram method¹⁹ and the CONTIN²⁰ method. However, great caution should be exercised in the interpretation of results, so that a picture emerges that is compatible with the physical reality.

In this paper we present an approach that is guided by the theoretical model of Semenov⁹, describing the time dependence of $g^{(1)}(t)$. In this model dynamic behaviour of polymers in the entangled regime, over various length and time scales, is rationalized in the framework of the reptation¹⁰ hypothesis in combination with the tube²¹ concept.

In the range $qL \leq 1$ (L is a characteristic length) the time-dependent correlation function of concentration and density fluctuations in semidilute and concentrated entangled polymer solutions can essentially be described by two different relaxation processes: a first fast cooperative stage (cooperative diffusion) and a second slow reptation-like stage.

(1) *Fast cooperative stage.* The cooperative diffusion process may be analysed with the aid of the two-fluid²²

model, where a semidilute solution is viewed as a transient network with a longitudinal elastic modulus E . The local velocity of the chains is du/dt and v is the velocity of the solvent continuum. The equation of motion of the network is governed by a balance between the friction force $c_m \zeta [(du/dt) - v]$ and the elastic restoring force $E \nabla^2 u$ expressed as:

$$c_m \zeta \left(\frac{du}{dt} - v \right) = E \nabla^2 u \quad (11)$$

The solution of equation (11) provides us with the relaxation time of a perturbation u_q with $\tau_{c,q \rightarrow 0} = 1/D_c q^2$, where c_m is the monomer concentration (number of monomers/volume) and the cooperative diffusion coefficient is given by:

$$D_c = E/c_m \zeta \quad (12)$$

The effective friction coefficient ζ is evaluated by dividing the 'blob' friction: $6\pi\eta\zeta$ (η is the solvent viscosity) by the number of monomers per 'blob' $c\xi^3$, i.e. $\zeta \approx 6\pi\eta/c_m \xi^2$. The quantity E is determined by the osmotic bulk modulus $K_{os} = c(\partial\pi/\partial c)$ and the shear modulus G through the relationship:

$$E = K_{os} + (4/3)G \quad (13)$$

The physical meaning of equation (12) is quite simple. The fluctuations of the network around its equilibrium position are in principle controlled by two driving forces encompassed by E , namely the osmotic contribution, which tends to equalize the concentration, and the elastic part which aims to keep the network in position. The fluctuations are damped by the friction force between the polymer network and the solvent. Since the functions K_{os} and G are both proportional to the number of contact points in the network, they should scale like $1/\xi^3$ and hence $E \propto 1/\xi^3$. Thus from the definition of ζ (see above) in combination with equation (12) we recover the familiar relation $D_c \propto \xi^{-1}$.

It is important to recognize that in cooperative diffusion all the polymer chains are collectively moving relative to the solvent and behave as an elastic 'sponge' moving in a viscous medium. In this process any disentanglement or large-scale motion of each chain will not be required during the process of motion, so the effect of topological constraints should not be essential. In light of this, it would not be surprising if the values of D_c for a solution and a gel of the same concentration are the same. There are d.l.s. measurements²³ which seem to support this presumption.

A basic constituent of the present approach is that the initial relaxation of $g^{(1)}(t)$ is characterized by a cooperative mode (cooperative diffusion coefficient). In this stage the decay of the correlation function may be described by a single exponential of the form:

$$g_c^{(1)}(t) = A_c \exp(-t/\tau_c) \quad (14)$$

where A_c is the reduced amplitude of the cooperative mode and τ_c is the cooperative relaxation time.

(2) *Slow reptation-like stage.* In the reptation-like mode, motion of individual polymer chains in entangled systems is considered. This process of motion can be anticipated to exhibit quite different features as compared with the cooperative mode. In this case, in contrast to the cooperative stage, topological constraints or the density of cross-links should be crucial for chain mobility.

The reptation model, incorporating the tube concept, has provided a fruitful and simple framework to analyse local chain dynamics. In this picture chain motion is considered by visualizing each chain as being confined in an effective 'tube' made of all topological constraints imposed on one chain by its neighbours. Since the chains cannot cross each other, each chain can only creep or 'reptate' in a snake-like fashion along the curvilinear axis of the tube, while any large-scale motion perpendicular to its local direction is hampered.

With the aid of the reptation model in combination with the tube hypothesis, Semenov constructed a model for the depiction of the time-dependent correlation function in entangled systems of flexible polymers. One of the main results from his analysis is that the relaxation of the correlation function in the reptation-like stage cannot be represented by a single exponential decay, but is characterized by a spectrum of relaxation times between T_{rep} and T_{max} . T_{rep} is estimated to correspond to a decrease of the reptation-like correlation function to roughly $1/e$. T_{max} is the longest time of conformational relaxation and is of the order of time needed for a polymer chain to fully creep out of the initial tube. The long-wave fluctuations in the reptation-like stage relax initially in the form of an exponential decay, followed ($t > T_{rep}$) by a decay giving rise to a long-lived 'tail'. The main part of the relaxation takes place during the time of order T_{rep} , while the remaining part relaxes during the time of order T_{max} , as a result of the smoothing out process of residual differences in the conformational state of the polymer chains. Roughly, we may argue that the reptation-like mode serves as a mechanism to relieve local constraints and thus further relax density fluctuations.

In order to model the situation outlined above, where we have a distribution of relaxation times, the empirical Williams–Watts exponential relaxation function²⁴ may be employed (no matter how broad the distribution is) to describe the correlation function associated with the reptation-like stage $g_{rep}^{(1)}(t)$. The function may be cast into the following form:

$$g_{rep}^{(1)}(t) = A_{rep} \exp[-(t/\tau_{rep,e})^\beta] \quad (15)$$

where A_{rep} is the amplitude of the reptation-like mode, $\tau_{rep,e}$ is some effective relaxation time, and $0 < \beta \leq 1$ is a measure of the width of the underlying distribution of relaxation times implied by the non-exponential character of the relaxation function. The average relaxation time for the Williams–Watts function is given by:

$$\tau_{rep} = (\tau_{rep,e}/\beta)\Gamma(1/\beta) \quad (16)$$

where $\Gamma(x)$ is the gamma function. Equation (15) allows a meaningful characterization of data on condition that the distribution of relaxation times is unimodal.

In this context it is interesting to note a recent semiempirical relaxation model²⁵, which is based on fundamentally different physical arguments to the reptation model, for the description of dynamics of entangled polymer systems. In the approach of Douglas and Hubbard the surmise is that material inhomogeneity may give rise to a situation where clusters of entangled chains move together, leading to a distribution of relaxation times associated with the cluster size distribution. From the theoretical analysis, a stretched exponential relaxation function emerges, of the form given by equation (15). In this model the exponent β is interpreted as a measure of material inhomogeneity and the specific value of β

depends on the topological dimension of the modelled cluster. We may note that the inhomogeneity model of Douglas and Hubbard is supported by a recent intensity light scattering study²⁶ of moderate concentrated polymer solutions, where enhanced low-angle scattering is attributed to the presence of inhomogeneities of the system.

Over the past years the Williams–Watts relaxation function has been demonstrated^{27–29} to be a powerful tool in analysing various relaxation phenomena in systems of entangled polymer chains. Great effort^{30,31} has been devoted in recent years to put this empirical function on a sound theoretical basis. For instance, Ngai and co-workers have developed a formalism^{32–34} to address the problem of how the relaxation of a ‘primitive’ mode is modified by coupling to complex surroundings. The fundamental prediction of the model is that initially the ‘primitive’ relaxation mechanism is slowed down exponentially due to environmental coupling and at longer times a non-exponential decay law of the Williams–Watts type follows.

In light of the above considerations we may now make the following proposal for the total time-dependent correlation function:

$$g_{\text{tot}}^{(1)}(t) = A_c \exp(-t/\tau_c) + A_{\text{rep}} \exp[-(t/\tau_{\text{rep}})^\beta] \quad (17)$$

In the model of Semenov the reduced amplitudes may be expressed as:

$$A_c = \frac{K_{\text{os}}}{K_{\text{os}} + E_G(0)}; \quad A_{\text{rep}} = \frac{\hat{E}}{K_{\text{os}} + \hat{E}} \quad (18)$$

with

$$\hat{E} = (8/15)E_G(0); \quad qR_G(c) \ll 1 \quad (19)$$

where $E_G(0)$ is the initial elastic modulus ($t \rightarrow 0$) of the entangled network and \hat{E} is an effective modulus.

EXPERIMENTAL

Materials and solution preparation

EHEC (Bermocoll CST-103) was manufactured by Berol Nobel AB, Stenungsund, Sweden and was from the same batch as previously used⁸. The viscosity average molecular weight for this sample was 150 000. The degree of substitution of ethyl groups was 1.5 per anhydroglucose unit, and molar substitution of ethylene oxide groups was 0.7 per anhydroglucose unit. The cationic CTAB was of analytical grade (Merck) and was used without further purification.

Desalted and purified EHEC solutions were prepared by dialysis against distilled water for 5 days. Hollow fibres made of regenerated cellulose were used as dialysing membrane (molecular cut-off at 6000; Spectrum Medical Industries). After freeze-drying, the polymer was redissolved in water. Samples were prepared by weighing the components and the solutions were homogenized by stirring at room temperature. The EHEC solutions were kept in a refrigerator for at least 1 week before the measurements were carried out, in order to ensure complete dissolution. For the system EHEC/CTAB/water, measurements on the two polymer concentrations of 0.15% (w/w) ($c < c^*$) and of 1.0 wt% ($c > c^*$), respectively, were performed. The concentration of the surfactant (CTAB) was 10 mmolal throughout, well above the critical concentration for formation of polymer-bound micelles. In addition, a solution of EHEC/water

with a concentration of 1.0 wt% was prepared. The solutions were filtered in an atmosphere of filtered air through, depending on concentration, 0.45 μm or 1.2 μm filters (Gelman Sciences) directly into pre-cleaned 10 mm n.m.r. tubes (Wilmad Glass Company) of highest quality.

Static and dynamic light scattering

In this work we used a standard, laboratory-built light scattering spectrometer capable of both absolute integrated scattered intensity and photon correlation measurements at different scattering angles. A Spectra Physics Model 2020 argon ion laser was operated at 488 nm, with vertically polarized light, and the output intensity of the beam was adjusted with the aid of high quality neutral density filters (Melles Griot) of various transmittances, depending upon the scattered light intensity level of sample solution. Polarizers were used both in front of and behind the cell in order to insure *vv* configuration. The sample cell was held in a thermostat block filled with silicone oil of matching refractive index, the temperature constancy being controlled to within $\pm 0.05^\circ\text{C}$.

In the static light scattering experiments, ALV light scattering electronics were used in combination with the on-line program ODIL. In the present experimental set-up we have used a detection geometry where a vertical slit, instead of a pinhole, is placed in front of the photomultiplier tube. With this arrangement the relationship between the excess scattered intensity I^* and the absolute quantity $R_{\text{VV}}(c, q)$ (cf. equation (2)) may be expressed as:

$$R_{\text{VV}}(c, q) = kI^*(c, q) \quad (20)$$

where

$$k = \frac{R_{\text{VV,benzene}} n_{\text{sol}}}{I_{\text{benzene}}^* n_{\text{benzene}}} \quad (21)$$

A value of $R_{\text{VV}}(90^\circ) = 3.14 \times 10^{-5} \text{ cm}^{-1}$ reported³⁵ for benzene at 25°C and 488 nm was employed in this study. Values of the function $[Hc/R_{\text{VV}}(c, q)]$ in the limit of $q = 0$ were determined from a Berry plot³⁶, that is, a plot of $[Hc/R_{\text{VV}}(c, q)]^{1/2}$ versus q^2 .

The normalized intensity autocorrelation function was measured at scattering angles of 60° and 90° with an ALV-5000 multiple tau digital correlator. The correlation functions were recorded in the real time ‘multiple tau’ mode of the correlator, in which 256 time channels are logarithmically spaced over an interval ranging from 0.2 μs to almost 1 h. First, a non-linear least-squares fitting algorithm (a modified Levenberg–Marquardt technique) was utilized to obtain best-fit values for the three parameters A_{rep} , τ_{rep} and β appearing in the second term on the right-hand-side of equation (17). By comparing the experimental correlation functions at different temperatures it is easy to find the part of the correlation functions representing the reptation-like mode. Afterwards the values of τ_{rep} and β were kept constant and the values of A_c and τ_c were determined by the fitting routine. In the fitting procedure we use the criterion that $A_c + A_{\text{rep}} = 1$.

RESULTS AND DISCUSSION

Let us first discuss the results obtained from the static light scattering measurements. In *Figure 1* the q^2 dependence of the normalized inverse scattered intensity

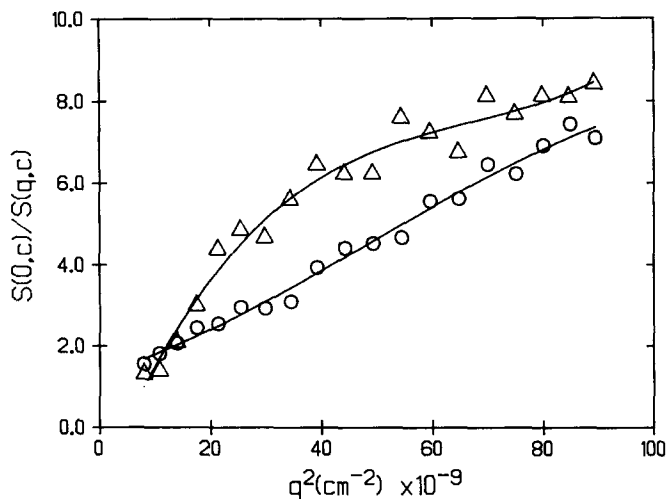


Figure 1 The q^2 dependence of the normalized inverse scattered intensity function for a dilute solution ($c = 0.15$ wt%) of the system EHEC/CTAB/water at temperatures: \circ , 25.0°C; \triangle , 43.3°C. The solid curves are only guides for the eye

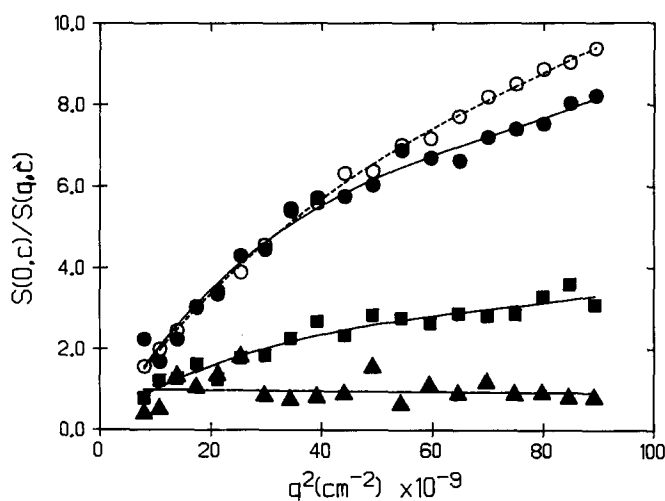


Figure 2 The q^2 dependence of the normalized inverse scattered intensity function for the semidilute system EHEC/CTAB/water ($c = 1.0$ wt%) at temperatures: \bullet , 25.0°C; \blacksquare , 34.5°C; \blacktriangle , 43.3°C, and for the semidilute system EHEC/water ($c = 1.0$ wt%) at 25.0°C (\circ). The solid curves are only guides for the eye

function for a dilute solution of the system EHEC/CTAB/water at two different temperatures, is illustrated. In view of equation (4) the results seem to indicate that the polymer molecules expand with increasing temperature. This finding corroborates with the recent surmise³⁷ that a temperature increase promotes the surfactant binding to the polymer. This should lead to coil expansion due to electrostatic repulsion between polymer-bound micelles. The tendency of curvature in the graph (Figure 1), representing data for the highest temperature, may be a sign of a conformational change.

Results for the same system in the semidilute regime are displayed in Figure 2 in the form $S(0, c)/S(q, c)$ versus q^2 . In this case the data for the highest temperature, at the gelation threshold, are practically independent of q^2 , while a progressively stronger q^2 dependence is observed with decreasing temperature. These features are attributed to enhanced binding of surfactant to the polymer chains with increasing temperature. The conjecture is that the

number of physical cross-links increases with temperature, hence the effective mesh size of the network is expected to be smaller (cf. equation (7)). This trend should lead to a weaker q^2 dependence of the ratio $S(0, c)/S(q, c)$ with increasing temperature. Figure 2 also shows data (at 25°C) for a solution of the same concentration (1.0 wt%), but without surfactant. These data show a somewhat stronger q^2 dependence than the corresponding data for the system with surfactant. This trend probably indicates that a certain degree of cross-linking has already been introduced at 25°C for the polymer-surfactant system. However, it should be mentioned that this system of EHEC/water exhibits strong turbidity effects at higher temperatures (the cloud point is located at about 30°C).

Let us now discuss the dynamic properties. Figure 3 shows correlation functions for the semidilute system EHEC/CTAB/water at the temperatures 24.9°C (sol) and 43.7°C (gel regime). A comparison of the correlation functions clearly reveals that there is a pronounced shift in the decay time towards higher values when the gel zone is approached. However, a thorough examination of the correlation function data will show that the initial relaxation (the cooperative stage) is practically the same for both temperatures, if the change of solvent viscosity with temperature is accounted for (see also below).

In Figure 4, experimental correlation functions for the semidilute sol-gel system at various temperatures, together with the corresponding curves fitted with the aid of equation (17), are depicted in the form of semilogarithmic plots. The experimental data are very well portrayed by the model represented by equation (17). This model facilitates a systematic analysis of the relaxation functions. All the correlation functions exhibit a common feature, namely the initial fast decay is characterized by a single exponential, followed by a long-time 'tail' described by the Williams-Watts non-exponential function with $\beta = 0.46 \pm 0.05$. The value of β was found to be constant, within experimental error, over the whole region from sol to gel. In a recent d.l.s. study on a covalently cross-linked silica system the Williams-Watts function was adopted to analyse correlation function data, and a value of $\beta = 0.66 \pm 0.05$ was reported³⁸. The model which was later developed³⁹ bears

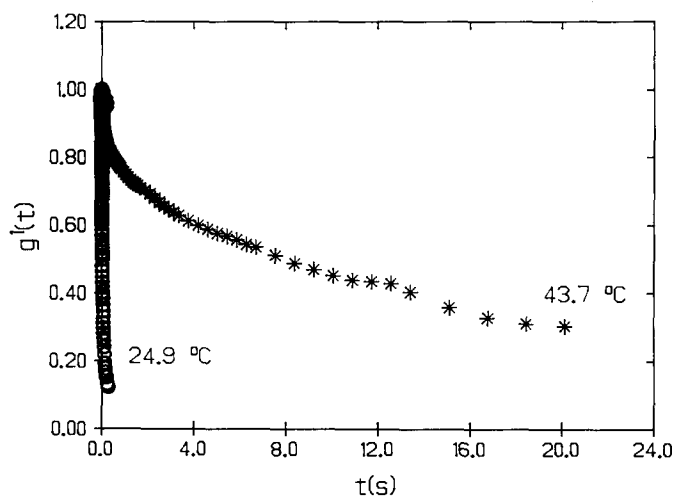


Figure 3 Plot of the first-order electric field correlation function as a function of time for the semidilute system EHEC/CTAB/water in the sol (24.9°C) and gel (43.7°C) states. Every second data point is shown. $\theta = 90^\circ$

a certain resemblance to the present approach. The difference in the value of β for these two systems probably indicates that the width of the distribution of decay times is related to the type of network formation mechanism involved.

Figure 5 depicts the temperature dependences of the cooperative and the reptation-like relaxation times, obtained from the fitting procedure of equation (17), for the semidilute polymer-surfactant system. A close inspection of the behaviour of τ_c indicates a weak decrease with temperature. This trend is probably a direct effect of the lower solvent viscosity with increasing temperature. The quantity τ_{rep} shows a very different pattern of behaviour. In this case the average relaxation time rises very strongly during the gelation process. This observation is consistent with the picture that the density of physical cross-links increases when the gel is formed. Thus the local motion of the chains forming the network is expected to be progressively slowed down when the gelation threshold is approached. Incidentally, we may remark that the same trend in the value of τ_{rep} (the long-time relaxation process) with temperature can be anticipated in the framework of the cluster model²⁵ mentioned above; in this case the average size of the formed clusters is expected to increase as the gelation process proceeds and hence longer relaxation times should be observed.

A close examination of the graph representing the temperature dependence of τ_{rep} in Figure 5 reveals a discernible transition zone. Figure 6 shows a magnification of this zone; the centre of the transition region is located at about 42°C. The same value can be inferred from viscoelastic measurements⁸ on the same system and at the same concentration, by comparing the temperature dependences of the shear storage modulus (G') and the shear loss modulus (G''). The transition where G'' becomes larger than G' occurs between 40 and 45°C, independently of the oscillation frequency. In this context it is interesting to note a recent d.l.s. study⁴⁰ on a thermoreversible gelling polysaccharide system. By plotting the slope obtained from the long-time 'tail' of the correlation function as a function of the temperature, a

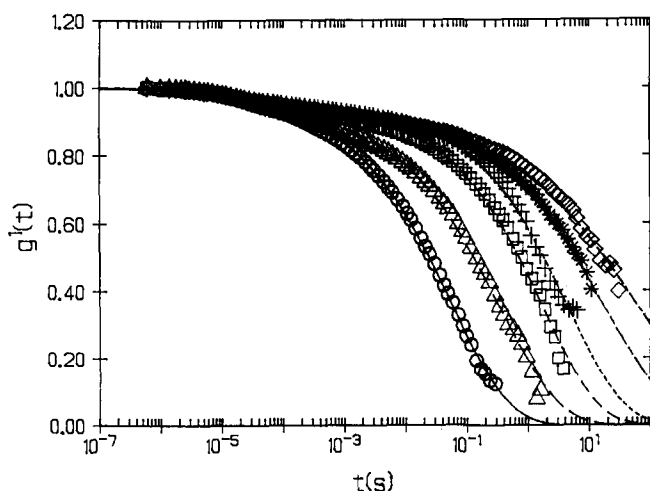


Figure 4 Plot of the first-order electric field correlation function as a function of time for the semidilute system EHEC/CTAB/water at temperatures (from sol to gel): \circ , 24.9°C; Δ , 32.2°C; \square , 35.8°C; $+$, 38.6°C; $*$, 45.7°C; \diamond , 51.0°C. Every second data point is shown. The curves are fitted with the aid of equation (17) (see text). $\theta = 90^\circ$

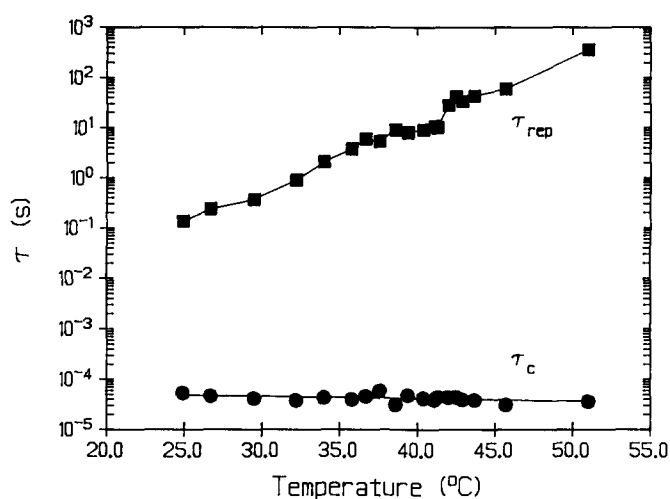


Figure 5 Temperature dependences of the cooperative (τ_c) and reptation-like (τ_{rep}) relaxation times for the semidilute system EHEC/CTAB/water. The values of τ_c and τ_{rep} have been obtained from a fitting procedure of equation (17) (see text). The solid curves are only guides for the eye

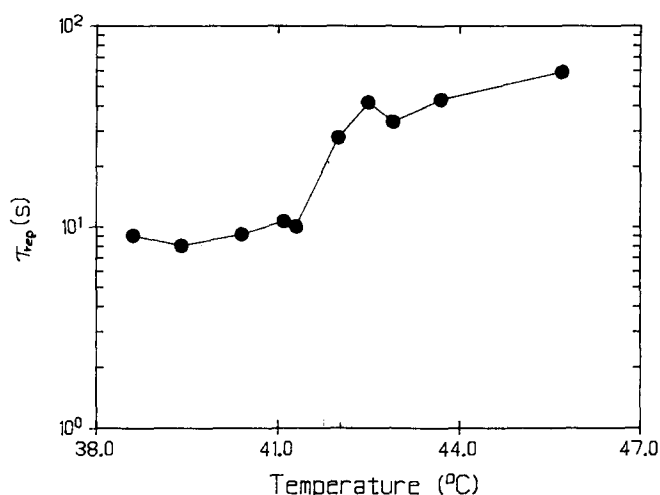


Figure 6 Plot of the reptation-like relaxation time as a function of temperature for the semidilute system EHEC/CTAB/water. This plot is a magnification of the transition zone of Figure 5 (see text). The solid curve is only a guide for the eye

sharp transition region was recognized with an inflection point identified as the gel point.

In Figure 7 the reduced amplitudes are plotted as a function of the temperature. We observe the large difference between the values of the two amplitudes. The approximate values are $A_{rep} \approx 0.95$ and $A_c \approx 0.05$. Judging from equation (18), the observed values of the amplitudes indicate that the factor $c \partial \pi / \partial c$ is small in comparison with $E_G(0)$ and \hat{E} . A rational explanation of this is that the thermodynamic conditions of the system are fairly poor, i.e. the second virial coefficient is small. The amplitudes exhibit only a weak temperature dependence.

In Figure 8 the correlation functions are displayed for a dilute and a semidilute solution of the system EHEC/CTAB/water, at a low and a high temperature. The small difference in decay rate between the correlation functions representing the dilute solution is probably correlated to the decrease in solvent viscosity with

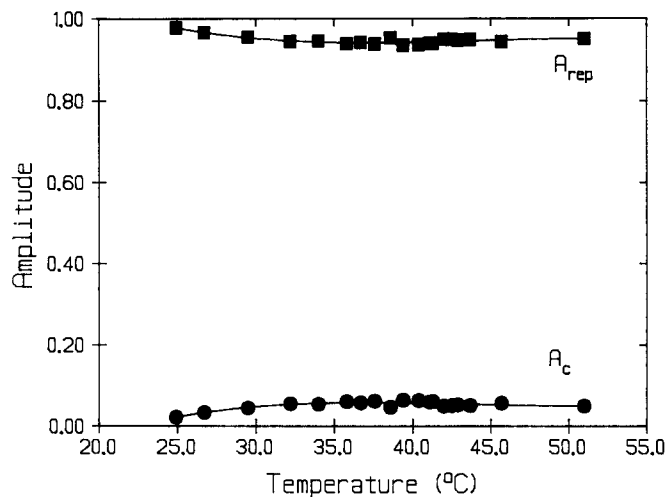


Figure 7 Plot of the reduced amplitudes (A_c and A_{rep}) as a function of temperature for the semidilute system EHEC/CTAB/water. The values of A_c and A_{rep} have been obtained from a fitting procedure of equation (17) (see text). The solid curves are only guides for the eye

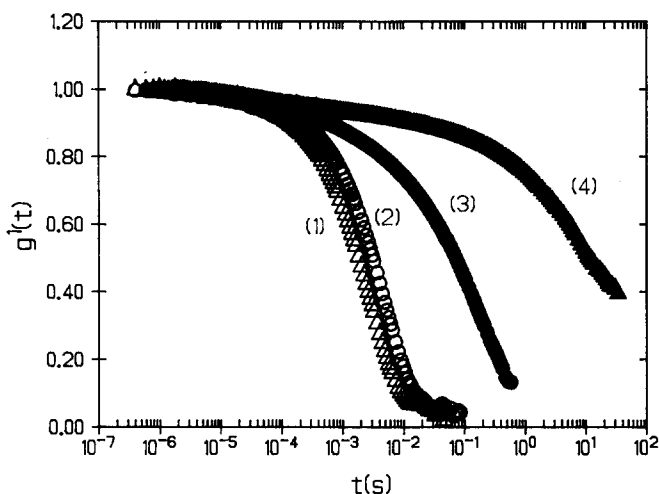


Figure 8 Plot of the first-order electric field correlation function as a function of time for the system EHEC/CTAB/water at concentrations and temperatures of: 1, $c = 0.15$ wt%, 43.4°C ; 2, $c = 0.15$ wt%, 25.0°C ; 3, $c = 1.0$ wt%, 25.0°C ; 4, $c = 1.0$ wt%, 43.6°C . $\theta = 60^\circ$

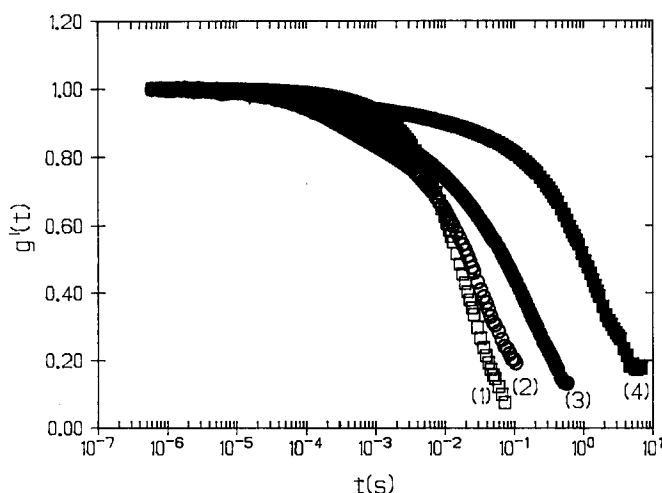


Figure 9 Plot of the first-order electric field correlation function as a function of time for semidilute systems ($c = 1.0$ wt%): 1, EHEC/water, 34.5°C ; 2, EHEC/water, 25.0°C ; 3, EHEC/CTAB/water, 25.0°C ; 4, EHEC/CTAB/water, 34.5°C . $\theta = 60^\circ$

temperature. For the semidilute system we observe the same marked temperature effect of the relaxation function as discussed above. These observations support the surmise that the long-time 'tail' of the correlation functions, as well as the ability of the system to form a gel, are features associated with the semidilute regime.

Correlation functions representing a semidilute system, with and without surfactant and at two different temperatures, are depicted in Figure 9. For the system without surfactant we notice only a slight difference in the relaxation, while for the system with surfactant a pronounced shift in the overall decay time towards higher values with increasing temperature is found. These observations strengthen the conjecture that the surfactant plays a key role for the marked change in dynamic behaviour discussed here. Finally, we may note that already at 25°C there is a significant difference between the decay times of the correlation functions representing the solution with and without surfactant. This finding indicates that incipient cross-linking effects of the network already take place at 25°C .

CONCLUSIONS

In this paper static and dynamic properties of a thermoreversible gelling system (EHEC/CTAB/water) have been studied by application of the light scattering technique. In dilute solution a coil expansion is observed with increasing temperature. This trend is attributed to enhanced surfactant binding to the polymer chains with temperature, leading to stronger electrostatic repulsion between polymer-bound micelles. In the semidilute regime the mesh size seems to become smaller during the gelation process. This effect is associated with a progressively stronger tendency of the system to create physical cross-links with increasing temperature.

The time-dependent correlation functions are probed over a temperature interval where the semidilute system (EHEC/CTAB/water) passes from a sol to a gel. The decay of the correlation function is shifted towards longer times with increasing temperature. This behaviour can be rationalized in the framework of a model where the decay of the correlation function is initially characterized by a single exponential (cooperative stage), followed by a long-time 'tail' described by a non-exponential Williams-Watts function. During the gelation process the relaxation of the cooperative mode is only slightly affected, whereas the long relaxation time exhibits a drastic change. The pronounced slowing down of the motion of individual chains when approaching the gelation threshold is associated with a reptation-like behaviour as a mechanism to relieve local constraints.

ACKNOWLEDGEMENTS

We thank G. Karlström, S. Nilsson, L. Piculell and H. Wennerström, Chemical Center, University of Lund, for stimulating discussions.

REFERENCES

- 1 Jones, M. N. *J. Colloid Interface Sci.* 1967, **23**, 36
- 2 Breuer, M. M. and Robb, I. D. *Chem. Ind.* 1972, **13**, 531
- 3 Leung, P. S., Goddard, E. D., Han, C. and Ginka, C. J. *Colloids Surf.* 1985, **13**, 47
- 4 Goddard, E. D. *Colloids Surf.* 1986, **19**, 255

- 5 Carlsson, A., Karlström, G. and Lindman, B. *Langmuir* 1986, **2**, 536
- 6 Carlsson, A., Karlström, G., Lindman, B. and Stenberg, O. *Colloid Polym. Sci.* 1988, **266**, 1031
- 7 Carlsson, A. PhD Dissertation, Lund University, 1989
- 8 Carlsson, A., Karlström, G. and Lindman, B. *Colloids Surf.* 1990, **47**, 147
- 9 Semenov, A. N. *Physica A* 1990, **166**, 263
- 10 De Gennes, P.-G. 'Scaling Concepts in Polymer Physics', Cornell University Press, Ithaca, 1979
- 11 Fujita, H. 'Polymer Solutions', Elsevier Science, Amsterdam, 1990
- 12 Mijnlieff, P. F. and Coumou, D. J. *J. Colloid Interface Sci.* 1968, **27**, 553
- 13 Farnoux, B. *Ann. Phys.* 1976, **1**, 73
- 14 Wiltzius, P., Haller, M. R., Cannell, D. S. and Schaefer, D. W. *Phys. Rev. Lett.* 1983, **51**, 1183
- 15 Okano, K., Wada, E., Kurita, K. and Fukuor, H. *J. Appl. Crystallogr.* 1978, **11**, 507
- 16 Siegert, A. J. F. Massachusetts Institute of Technology Rad. Lab. Rep. No. 465, 1943
- 17 Arfken, G. 'Mathematical Methods for Physicists', Academic Press, New York, 1970
- 18 Koppel, D. E. *J. Chem. Phys.* 1972, **57**, 4814
- 19 Chu, B., Gulari, E. and Gulari, E. *Phys. Scr.* 1979, **19**, 476
- 20 Provencher, S. W. *Makromol. Chem.* 1979, **180**, 201
- 21 Doi, M. and Edwards, S. F. 'The Theory of Polymer Dynamics', Oxford University Press, Oxford, 1986
- 22 Borchard, F. and de Gennes, P.-G. *Macromolecules* 1977, **10**, 1157
- 23 Munch, J. P., Candau, S., Herz, J. and Hild, G. *J. Phys. (Paris)* 1977, **38**, 971
- 24 Williams, G. and Watts, D. C. *Trans. Faraday Soc.* 1970, **66**, 80
- 25 Douglas, J. F. and Hubbard, J. B. *Macromolecules* 1991, **24**, 3163
- 26 Medjahdi, G., Sarazin, D. and François, J. *Macromolecules* 1991, **24**, 4138
- 27 Patterson, G. D. *Adv. Polym. Sci.* 1983, **48**, 125
- 28 Fytas, G. in 'Physical Optics and Dynamic Phenomena in Macromolecular Systems' (Ed. B. Sedláček), W. de Gruyter, Berlin, 1985, p. 205
- 29 Patterson, G. D. in 'Dynamic Light Scattering' (Ed. R. Pecora), Plenum, New York, 1985, p. 245
- 30 Shore, J. E. and Zwanzig, R. *J. Chem. Phys.* 1975, **63**, 5445
- 31 Budimir, J. and Skinner, J. L. *J. Chem. Phys.* 1985, **82**, 5232
- 32 Rendell, R. W., Ngai, K. L. and McKenna, G. B. *Macromolecules* 1987, **20**, 2250
- 33 Ngai, K. L., Rendell, R. W., Rajagopal, A. K. and Teitler, S. *Ann. N.Y. Acad. Sci.* 1985, **484**, 150
- 34 Ngai, K. L., Rajagopal, A. K. and Teitler, S. *J. Chem. Phys.* 1988, **88**, 5086
- 35 Chu, B., Onclin, M. and Ford, J. R. *J. Phys. Chem.* 1984, **88**, 6566
- 36 Berry, G. C. *J. Chem. Phys.* 1966, **44**, 4550; 1967, **46**, 1338
- 37 Carlsson, A., Karlström, G. and Lindman, B. *J. Phys. Chem.* 1989, **93**, 3673
- 38 Martin, J. E. and Wilcoxon, J. P. *Phys. Rev. Lett.* 1988, **61**, 373
- 39 Martin, J. E., Wilcoxon, J. P. and Odinek, J. *Phys. Rev. A* 1991, **43**, 858
- 40 Lang, P. and Burchard, W. *Macromolecules* 1991, **24**, 814